RAPID COMMUNICATIONS

PHYSICAL REVIEW B **82**, 121401(R) (2010)

Impact of disorder on the $\nu=2$ quantum Hall plateau in graphene

Jean-Marie Poumirol, Walter Escoffier, Amit Kumar, Bertrand Raquet, and Michel Goiran
Laboratoire National des Champs Magnétiques Intenses, INSA UPS, CNRS UPR 3228, Université de Toulouse, 143 avenue de Rangueil, 31400 Toulouse, France
(Received 4 June 2010; revised manuscript received 13 July 2010; published 1 September 2010)

We investigate the quantum Hall regime in a graphene flake with different levels of disorder. Under high magnetic field, an unexpected decrease in the Hall resistance occurs when only the zeroth-energy Landau level is populated. The presence of disorder rules out the expected appearance of the $\nu=0$ quantum Hall plateau as in the case of pristine graphene. Instead, we propose an alternative explanation based on the coexistence of two types of carriers, electrons and holes, induced by high magnetic field, in the presence of disorder.

DOI: 10.1103/PhysRevB.82.121401 PACS number(s): 73.43.−f, 72.20.My, 72.80.Vp

Graphene, has generated extended experimental and theoretical works during the last few years in order to explore the unique properties of massless Dirac fermions.[1–4] In clean graphene, at very high magnetic field, spin and valley degeneracy lifting has been unveiled with conductance plateaus at filling factors corresponding to $\nu=0,\pm1,\pm4$.[5,6] Such broken-symmetry states are theoretically addressed in the frame of quantum Hall ferromagnetism[7] or the formation of excitonic energy gaps.[8] It is worth mentioning that, while the $\nu=\pm1$ and ±4 plateaus are experimentally visible in both Hall resistance and conductance, the $\nu=0$ state responsible for the divergence of the longitudinal resistivity remains poorly investigated through Hall resistance measurements, except in recent works.[9–11] In addition to experimental issues concerning the accurate measurement of the vanishing Hall component combined with the divergent longitudinal resistance, the presence of disorder, resulting in spatial inhomogeneity of carriers certainly plays a crucial role on the onset of the zero-resistance Hall plateau.[12] A long-range potential disorder is already well known to alter the divergence of the longitudinal magnetoresistance at the charge neutrality point (CNP).[13]

In the following, we experimentally address the impact of disorder on the Hall quantization in a graphene flake, up to 60 T. We observe a large decrease in the absolute value of the Hall resistivity from the $\nu=\pm2$ plateau to a value close to zero. The onset of the Hall resistance decrease occurs at a constant filing factor for a given level of disorder. A careful analysis shows that this behavior cannot be supported by the emergence of the $\nu=0$ quantum Hall plateau. We propose an alternative explanation based on the coexistence of electrons and holes as a consequence of the magnetic field induced Fermi energy shift in a disordered electrostatic potential landscape.

The graphene sample was obtained by the standard mechanical exfoliation method of bulk graphite on a 300-nm-thick SiO_2 layer grown on a doped Si substrate. The sample has been etched into a Hall bar of size 3×1 μm^2 (form factor of 3). The contacts of typical size 1×1 μm^2 display ohmic behavior with a resistance per contact estimated to 1 kΩ. The Fermi level was tuned by applying a backgate voltage. The resistance of the device before and after annealing is shown in Fig. 1. The annealing procedure consists in a 12 h heating at 360K under vacuum (10^{-5} mbar). For clarity, the sample will be named S1 before annealing and S2 once annealed. For sample S1, the gate voltage corresponding to the CNP is 52 V and the field effect mobility deduced from the $R(V_g)$ curve is estimated to 0.13 $m^2/V\,s$;[14] for sample S2, the CNP is located at 3 V and the mobility is increased up to 0.35 $m^2/V\,s$. These mobility values are consistent with the Hall mobilities. The annealing process deeply modifies the conduction properties, by removing part of doping elements adsorbed at the sample surface or in its vicinity. At low carrier density, close to the CNP, the remaining charged impurities lead to an inhomogeneous electron/hole puddle landscape.[15] The residual carrier density at the minimum of conductivity induced by charged impurities evolves from $n_0=7.5\times10^{15}$ m^{-2} for S1 to $n_0=1.7\times10^{15}$ m^{-2} for S2. The backgate voltage range (ΔV_g), where electrons and holes coexist scales with the shift of the CNP from the zero backgate value.[16] Here, ΔV_g equals 20 V and 5 V for S1 and S2, respectively. This is fully consistent with the theoretical predictions given by $\Delta V_g=2n_0/C_g$, assuming the residual carrier densities deduced from Fig. 1 and an electrostatic backgate efficiency $C_g=7.2\times10^{10}$ $cm^{-2}\,V^{-1}$.[16] Note that other sources of disorder, such as vacancies, charged impurities trapped into the silicon oxide or ripples, are much more robust and cannot be removed by this method. Hall and longitudinal resistances are simultaneously measured under a

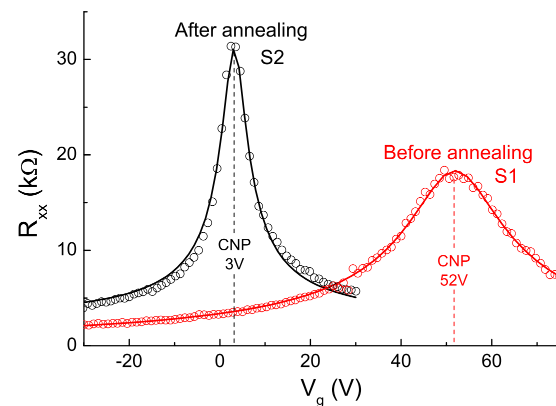

FIG. 1. (Color online) Four-probe longitudinal resistance versus backgate voltage, before and after annealing (S1 and S2, respectively), measured at 1.6 K. Solid lines are the theoretical fits (Ref. 14) from which we extract the mobility and the residual carrier concentrations at the CNP.

 ©2010 The American Physical Society

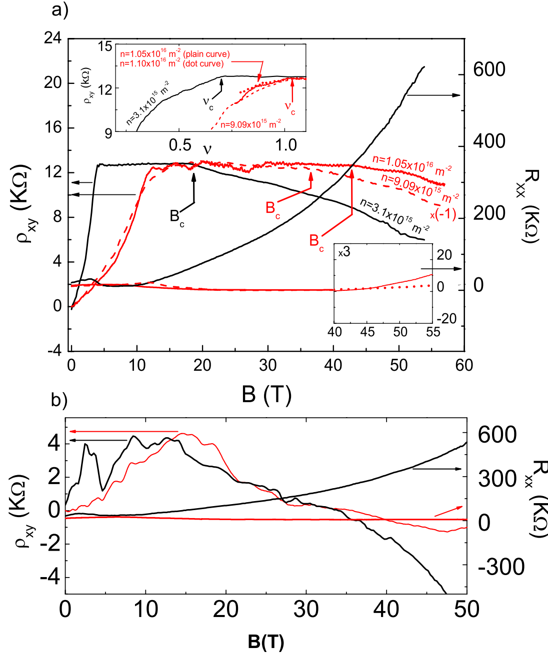

FIG. 2. (Color online) (a) $\rho_{xy}(B)$ and $R_{xx}(B)$ of S1 and S2 for different electrostatically doped states. The black plain curves stand for S2 at V_g=0 V and n=3.1×10^{15} m^{-2}. The plain red (dark gray) curves stand for S1 at V_g=40 V and n=1.05×10^{16} m^{-2} while the dash red (dark gray) curves stand for S1 at V_g=60 V and n=9.09 ×10^{15} m^{-2}. Lower right inset: zoom of $R_{xx}(B)$ (×3) between 40 and 55 T for S1. Upper left inset: the same ρ_{xy} curves plotted as a function of the filling factor $\hbar/(eB)$, with an additional doping level at V_g=65 V and n=1.1×10^{16} m^{-2} for S1 represented by the dot red (dark gray) curve. (b) $\rho_{xy}(B)$ and $R_{xx}(B)$ at the CNP for S1 and S2, red (dark gray) and black curves, respectively.

transverse magnetic field at 1.6 K and over a wide range of backgate voltage.

Figure 2 reports on magnetotransport measurements for S1 and S2 at 1.6 K in the electrostatically doped states [Fig. 2(a)] and at the CNP [Fig. 2(b)]. The main panel of Fig. 2(a) shows the Hall resistivity $\rho_{xy}(B)$ and the longitudinal magnetoresistance $R_{xx}(B)$, of sample S1 at different carrier densities in both electron and hole regimes as well as for sample S2 in the hole regime. Under these strong doping conditions, only one type of carriers participates to the conduction, as confirmed by the linear Hall voltage at low magnetic field. In the high magnetic field regime, we observe for each doping the expected quantized Hall plateau, corresponding to the filling factor $\nu=\pm 2$. However, the plateau is stable up to a magnetic field marked by the arrows in Fig. 2, above which the absolute value of the Hall resistance starts to decrease slowly. Meanwhile, the longitudinal resistance of the sample S2 is drastically increased by the applied magnetic field [black curve, Fig. 2(a)]. Conversely, for S1, $R_{xx}(B)$ remains nearly constant all over the explored magnetic field range. The lower right inset of Fig. 2(a) is a zoom (×3) of $R_{xx}(B)$ obtained for S1 between 40 and 55 T. One notes that despite the larger increase in $R_{xx}(B)$ at V_g=40 V compared to V_g=60 V, the Hall resistance decrease takes place at a higher magnetic field for V_g=40 V. In the upper left inset of Fig. 2(a), ρ_{xy} is plotted as a function of the filling factor $\nu=nh/(eB)$ for different carrier concentrations. The values of ν, where the Hall resistance starts to deviate from the quantized plateau are clearly visible due to a large variation in the $R_{xy}(\nu)$ slope. We easily extract a threshold filling factor ν_c, below which the Hall resistance decreases. The extracted values of ν_c for S1 range between 1.00 and 1.03 while it reads 0.71 for S2. Thus, for sample S1, the departures of the Hall resistance from the plateau value start at similar values of Fermi energy with respect to the Landau levels (LLs). On the other hand, ν_c seems to be related to the disorder strength in a direct way: a stronger disorder induces a decrease in the Hall resistance plateau at lower magnetic field.

Figure 2(b) reports on the magnetotransport measurements at the CNP. The two Hall curves for S1 and S2 exhibit qualitatively the same behavior: (i) a nonlinear increase at low magnetic field, which is the signature of a two carriers driven conduction, holes being slightly majority, (ii) after reaching a maximum, the Hall resistivity decreases and shows a sign reversal between 36 and 40 T for the two samples. On the other hand, the longitudinal magnetoresistance curves are drastically different with a strong increase in the resistance for S2 and an almost field independent behavior for S1. One can note that large fluctuations are present up to moderate magnetic field on the $\rho_{xy}(B)$ curves. These fluctuations have already been seen and explained in term of a percolation process across an electron and hole puddle landscape.[17,18]

Some comments can be mentioned from the above description: first, the lower value of ν_c on the cleanest sample is inconsistent with the onset of the degeneracy lifting of the n=0 LL. Indeed, the broadening of the LLs due to a higher disorder rate should shift the degeneracy lifting onset toward stronger magnetic fields. Second, we do not observe any correlation between the decrease in the Hall resistivity and the strong increase in $R_{xx}(B)$.[12] Besides, the Hall resistivity does not unveil a plateau at zero ohm but a sign reversal that demonstrates a change in majority carriers. Again, these experimental facts rule out the degeneracy lifting of the n=0 LL contribution and call for an alternative explanation based on the magnetic dependence of the relative electron and hole densities.

To explore deeper the magnetic field influence on the carrier concentration, we perform Hall measurements at various backgate voltages close to the CNP, into the electrons and holes coexistence region, for S1 [Fig. 3(a)]. The decrease in the absolute value of the Hall resistance at high magnetic field is observed for any backgate voltage and is almost symmetrical for holes and electrons. The two-dimensional (2D) color map of Fig. 3(b) summarizes all the data obtained on S1 and represents the variations in the Hall resistivity versus the gate voltage and the magnetic field. The red and blue areas (both dark gray areas) correspond to the Hall plateaus at ν=2 and ν=−2, respectively. The green (light gray) zone is related to the coexistence zone of both electrons and holes with an Hall resistance lower than $\pm h/2e^2$. We clearly observe a significant increase in the coexistence zone above 26 T, delimited by dashed lines. To quantitatively describe the magnetic field dependence of the relative electrons and holes density, we define $\alpha=(n_h-n_e)/(n_h+n_e)$, where $n_e(n_h)$ is the concentration of electrons (holes). In Fig. 3(c) are plotted the

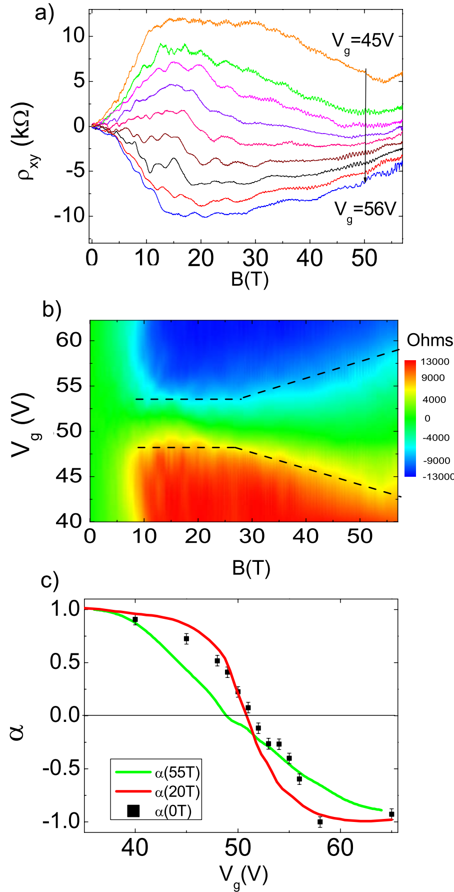

FIG. 3. (Color online) (a)$R_{xy}(B)$ measured in the vicinity of the CNP for S1, V_g varying from 45 to 56 V by step of 1 V. (b) The corresponding color (grayscale) map of $R_{xy}(B,V_g)$. The dashed lines are guide to the eyes that delimit the electrons and holes coexistence zone in the quantum regime. (c) $\alpha(V_g)$ curves at 0, 20 and 55 T.

$\alpha(V_g)$ curves obtained at 0, 20, and 55 T. At zero field, $\alpha(V_g)$ is deduced from the low-field part of the $\rho_{xy}(B)$ curves using the standard two fluid model.[19,20] The $\alpha(V_g)$ curves at 20 and 55 T are determined by considering that at such fields, all the carriers are distributed in the $n=0$ Landau state and no degeneracy lifting has occurred yet. So, the ratio α can simply be expressed by $\alpha(V_g,B)=2\rho_{xy}(V_g,B)e^2/h$. Across the CNP, we remark a smoother transition from holes to electrons in high-field regime as well as a small decrease in the backgate voltage corresponding to the CNP, from 52 V at zero field to 49 V at 55 T. For this sample, these features highlight a noticeable change in the electron-hole ratio induced by a magnetic field higher than 30 T

We interpret the Hall resistivity behavior as fingerprint of an inhomogeneous system composed by electron and hole puddles under a strong magnetic field. The upper part of Fig. 4(a) is a schematic view of the sample surface with blue and red dots (dark-gray dots) representing the long-range potential scatterers due to charged impurities of opposite signs. The lower part of Fig. 4(a) illustrates the spatial modulation of the zero-energy level in presence of these impurities.[21]

When a magnetic field is applied perpendicular to the disordered graphene flake, the quantization of the cyclotron orbits goes along with the onset of spatially segregated Landau states, with different zero energies (E_0), following the CNP landscape.[12]

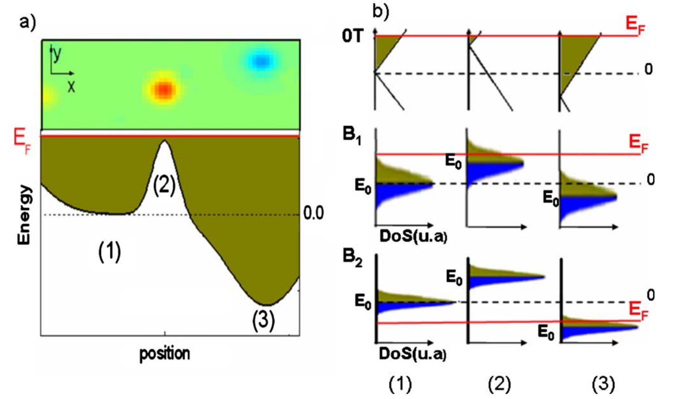

FIG. 4. (Color online) (a) Upper part: a 2D color scheme representing the electric potential of the sample. The green color (light gray) is for neutral zone whereas the charged impurities are revealed by blue or red dots (dark-gray dots) depending on their sign. Lower part: the spatial modulation of the zero energy due to the Coulomb potential induced by the charge impurities. The red (dark gray) line indicates an arbitrary Fermi level in case of an electron-doped sample. The black dot line is the zero-energy level for a pristine graphene flake. The annotations (1), (2), and (3) pinpoint selected zones which are electron doped, hole doped, and neutral, respectively. (b) DoS at zero energy for the three selected zones under increasing magnetic fields. The Fermi energy level is marked by the red (dark-gray) line and is downshifted when increasing the magnetic field.

Except for the zero-energy LL, the higher energy Landau states are upshifted by the magnetic field and lie above the Fermi level. At ν=2, only the $n=0$ LL remains below E_F. Figure 4(b) proposes an illustration of the magnetic field dependence of the density of states (DoS) for three arbitrary zones of the sample, which are electron doped (3), hole doped (2), and neutral (1), according to the charge impurities Coulomb potential depicted in Fig. 4(a). The Fermi energy is fixed in such a way that, at zero field, only electrons are present in the system.[22] The magnetic field B_1 is assumed high enough to ensure that all the charge carriers are distributed into the $n=0$ LL for the three areas. This sketch is obtained following the three basic assumptions: (i) the energies of the $n=0$ LLs, referred to as E_0, are insensitive to the magnetic field and are only determined by the local electrical potential of the sample, (ii) the DoS of the spatially segregated $n=0$ LLs increases with the magnetic field, and (iii) the Fermi level is uniform in the sample. When the magnetic field is increased from B_1 to B_2 [Fig. 4(b) and 4(c)], the Fermi energy is downshifted to accommodate the increase in the DoS at E_0 for the three zones. For a large magnetic field (B_2), the Fermi energy lies below E_0 for the two first zones (1) and (2), and converges to the lowest zero-energy level of the third zone that provides enough available electronic states to accommodate all the electrons. The straightforward consequence is the appearance of hole states above the Fermi level into the zones (1) and (2). These populated hole states have a direct impact on the Hall effect: the two types of

carriers are now present in the system, which is revealed by a decrease in the Hall resistance in the very high magnetic field regime [see Fig. 2(a)]. In this scheme, the magnetic field induced holes and electrons coexistence is directly related to the disorder characteristics of the sample. This explains the unique threshold filling factor ν_c we experimentally observe whatever the carriers concentration at zero field for a given disorder [upper inset Fig. 2(a)]. This scenario also validates the lower ν_c value once the strength of the disorder is significantly reduced. In the vicinity of the CNP, when electrons and holes coexist at zero field, the proposed explanation remains valid and the magnetic field tends to equilibrate the two carriers densities.

One notes that the small shift of the CNP with the magnetic field [Fig. 3(c)] is unexpected. This unveils a weak asymmetry between holes and electrons at low energies. One may invoke the local doping at the contacts, where the effect of the magnetic field is certainly less efficient. Complementary experiments are required to understand the charge neutrality shift under large magnetic field.

In conclusion, we report a nonconventional behavior of the quantum Hall effect in a graphene monolayer under very high magnetic field. The Hall resistance decrease at $\nu=\pm 2$ has been studied as function of the carrier concentration and the disorder level for a same sample. We give evidence that the disorder rate (more precisely its energy spreading) drives the magnetic field induced modification of the relative electron and hole densities by providing occupied electronic (hole) states below (above) the Fermi energy. These levels originate from the local fluctuations of the electrical potential across the sample. They become accessible thanks to the shift of the Fermi energy which accommodates the strong increase in the density of states of the $n=0$ LLs, under a large magnetic field. This work demonstrates the emergence of a different transport regime induced by disorder in graphene under high magnetic field. In very clean graphene, such a regime cannot be observed since the amplitude of the electrical potential fluctuations across the sample is smaller than the $n=0$ LL degeneracy lifting energy scales.

We would like to thank K. S. Novoselov for providing sample. We are also indebted to A. Cresti for valuable comments and remarks. Part of this work has been supported by EuroMagNET II under EU Contract No. 228043 and the French National Agency for Research (ANR) under Contract No. ANR-08-JCJC-0034-01.

[1] K. Novoselov, A. Geim, S. Morozov, D. Jiang, M. Katsnelson, I. Grigorieva, S. Dubonos, and A. Firsov, Nature (London) **438**, 197 (2005).

[2] Y. Zhang, Y. Tan, H. Stormer, and P. Kim, Nature (London) **438**, 201 (2005).

[3] A. K. Geim and K. S. Novoselov, Nature Mater. **6**, 183 (2007).

[4] A. H. Castro Neto, F. Guinea, N. M. R. Peres, K. S. Novoselov, and A. K. Geim, Rev. Mod. Phys. **81**, 109 (2009).

[5] Y. Zhang, Z. Jiang, J. P. Small, M. S. Purewal, Y. W. Tan, M. Fazlollahi, J. D. Chudow, J. A. Jaszczak, H. L. Stormer, and P. Kim, Phys. Rev. Lett. **96**, 136806 (2006).

[6] Z. Jiang, Y. Zhang, H. L. Stormer, and P. Kim, Phys. Rev. Lett. **99**, 106802 (2007).

[7] K. Nomura and A. H. MacDonald, Phys. Rev. Lett. **96**, 256602 (2006).

[8] V. P. Gusynin, V. A. Miransky, S. G. Sharapov, and I. A. Shovkovy, Phys. Rev. B **74**, 195429 (2006).

[9] M. Amado, E. Diez, D. López-Romero, F. Rossella, J. Caridad, V. Bellani, and D. Maude, New J. Phys. **12**, 053004 (2010).

[10] A. J. M. Giesbers, U. Zeitler, L. A. Ponomarenko, R. Yang, K. S. Novoselov, A. K. Geim, and J. C. Maan, Phys. Rev. B **80**, 241411(R) (2009).

[11] A. J. M. Giesbers, L. A. Ponomarenko, K. S. Novoselov, A. K. Geim, M. I. Katsnelson, J. C. Maan, and U. Zeitler, Phys. Rev. B **80**, 201403 (2009).

[12] S. Das Sarma and K. Yang, Solid State Commun. **149**, 1502 (2009).

[13] J. G. Checkelsky, L. Li, and N. P. Ong, Phys. Rev. B **79**, 115434 (2009).

[14] S. Kim, J. Nah, D. Shahrjerdi, L. Colombo, Z. Yao, E. Tutuc, and S. K. Banerjee, Appl. Phys. Lett. **94**, 062107 (2009).

[15] J. Martin, N. Akerman, G. Ulbricht, T. Lohmann, J. Smet, K. Klitzing, and A. Yacoby, Nat. Phys. **4**, 144 (2008).

[16] S. Adam, E. Hwang, V. Galitski, and S. D. Sarma, Proc. Natl. Acad. Sci. U.S.A. **104**, 18392 (2007).

[17] J. Poumirol, W. Escoffier, A. Kumar, M. Goiran, B. Raquet, and J. Broto, New J. Phys. **12**, 083006 (2010).

[18] A. Rycerz, J. Tworzydlo, and C. Beenakker, EPL **79**, 57003 (2007).

[19] S. Cho and M. S. Fuhrer, Phys. Rev. B **77**, 081402 (2008).

[20] E. H. Hwang, S. Adam, and S. Das Sarma, Phys. Rev. B **76**, 195421 (2007).

[21] P. Gallagher, K. Todd, and D. Goldhaber-Gordon, Phys. Rev. B **81**, 115409 (2010).

[22] P. Dietl, G. Metalidis, D. Golubev, P. San-Jose, E. Prada, H. Schomerus, and G. Schon, Phys. Rev. B **79**, 195413 (2009).